Biophysical *Journal*
Article

Biophysical Society

Reentrant Efficiency of Phototaxis in *Chlamydomonas reinhardtii* Cells

Sujeet Kumar Choudhary,[1] Aparna Baskaran,[2] and Prerna Sharma[1,*]
[1]Department of Physics, Indian Institute of Science, Bengaluru, Karnataka, India and [2]Martin A. Fisher School of Physics, Brandeis University, Waltham, Massachusetts

ABSTRACT Phototaxis is one of the most fundamental stimulus-response behaviors in biology wherein motile microorganisms sense light gradients to swim toward the light source. Apart from single-cell survival and growth, it plays a major role at the global scale of aquatic ecosystems and bioreactors. We study phototaxis of single-celled algae *Chlamydomonas reinhardtii* as a function of cell number density and light stimulus using high spatiotemporal video microscopy. Surprisingly, the phototactic efficiency has a minimum at a well-defined number density, for a given light gradient, above which the phototaxis behavior of a collection of cells can even exceed the performance obtainable from single isolated cells. We show that the origin of enhancement of performance above the critical concentration lies in the slowing down of the cells, which enables them to sense light more effectively. We also show that this steady-state phenomenology is well captured by modeling the phototactic response as a density-dependent torque acting on an active Brownian particle.

SIGNIFICANCE Phototaxis is one of the most fundamental stimulus-response behaviors in biology, and it plays a major role at the global scale of aquatic ecosystems and bioreactors. We study phototaxis of single-celled algae *Chlamydomonas reinhardtii* using high spatiotemporal video microscopy. Surprisingly, the phototactic efficiency has a minimum at a well-defined cell density, above which the phototaxis behavior of collections of cells even exceeds the performance obtainable from single isolated cells. We show that this collective enhancement originates from a density-dependent slowing down of the swim speed. Our results demonstrate a simple physical mechanism underlying the observed collective phototaxis of *Chlamydomonas* cells and can serve as a paradigm for the analysis of collective motility and taxis in microorganisms, in general.

INTRODUCTION

Collective behavior is observed in biological systems at different levels of biological organization from cells in tissues to colonies of microorganisms to flocks or herds of macroscopic animals (1–3). Phenomena at the level of the population in such systems cannot always be predicted by simply knowing the behavior of individuals. For example, biofilms of *Bacillus subtilis* bacteria exhibit oscillatory growth rate, whereas no such oscillations exist in dilute suspensions of the same bacteria (4). Collective behavior in microorganisms is of particular interest because it can be thought of as a precursor to multicellularity and more complex organizations of living systems. Consequently, a number of quantitative studies have recently elucidated the origin of collective phenomena in a wide variety of microorganisms such as *Escherichia coli* (5,6), *Bacillus subtilis* (4,7,8), *Synechocystis sp* (9,10), *Pseudomonas* (11,12), and *Myxococcus xanthus* (13,14).

Taxis, a transport phenomenon in which organisms undergo directed movement in response to a stimulus or a nutrient gradient, provides a particularly tractable context in which to explore collective behavior. As a particular example, phototactic cells such as algae and cyanobacteria respond to light gradients (15–17). Single-celled eukaryotic algae *Chlamydomonas reinhardtii* (CR) is a model biological organism for studying phototaxis (18). While single-cell response of CR to light can be tuned by varying physical variables such as light intensity, fluid viscosity as well as through chemical variables such as extracellular calcium concentration (16,19–22), it was shown recently that phototaxis of dense suspensions of CR was governed by the cell number density itself revealing that collective effects could modulate the single-cell response (23). Here, we setup

Submitted April 23, 2019, and accepted for publication September 9, 2019.
*Correspondence: prerna@iisc.ac.in
Editor: Vivek Shenoy.
https://doi.org/10.1016/j.bpj.2019.09.016

quasi-two-dimensional (2D) phototaxis assay with CR to study the crossover from the individual to collective phototaxis and identify the mechanisms underlying the emergence of its collective phototaxis.

CR has two flagella and an eyespot located near the cell equator. Its flagella move in breast-stroke fashion to propel the cell body through the fluid (18,24). The ellipsoidal-shaped cell body rotates about its own axis while swimming, enabling the eyespot to scan the incident light around the swimming path (25–27). Under phototactic light exposure, beating of the flagellum closest to the eyespot is inhibited, whereas beating of the farther away one is enhanced resulting in aligning the cell toward the light source (28,29). We use a high-speed camera to record individual trajectories of hundreds of cells under varying light intensities and cell concentrations.

We find that starting from a few cells per unit volume, phototactic efficiency decreases with increasing cell concentration until a critical concentration is reached, above which the efficiency increases with increasing concentration. Thus, the phototactic efficiency is a reentrant function of the cell density. We further show that the origin of this reentrant behavior lies in the decrease in the swim speed of the cells as density increases beyond the critical concentration. Finally we find that the observed phenomenology is well captured by a model of active Brownian particles subject to a density-dependent external torque.

MATERIALS AND METHODS

CC-1690 (wild-type) cells were used for the experiment. Synchronous cultures of CR were grown in TAP media at 25°C on a 12 h/12 h light/dark cycle in an orbital shaker (135 rpm). Fig. 1 *a* shows a schematic of the experimental setup. Cell suspension was observed in rectangular quasi-2D chambers (50 mm × 5 mm × 66 μm) made of glass slide and coverslip with double-sided tape as a spacer. A blue laser beam of wavelength 488 nm from the optical fiber illuminated one end of the chamber to act as a stimulus for phototaxis (Fig. S1). Cell trajectories were imaged using bright-field imaging with red light (760 nm and above) illumination setup on an Olympus IX73 inverted microscope (Tokyo, Japan). Images were recorded at 100 frames per second at 10× magnification using PCO 1200 hs CMOS camera coupled to the microscope. A 10× objective has a large depth of focus that enables us to capture 2D projections of the cell trajectories for as long as typically ∼20 s. Particle tracking was performed using image processing codes in MATLAB (The MathWorks, Natick, MA) and Python. For a given cell concentration and light intensity, 500–2500 trajectories were analyzed to have robust statistics. Cell trajectories were recorded using polarization microscopy at 33 frames per second with high magnification (40×) in pitch-dark condition to determine the frequency of the cell body rotation. The eyespot of the cell appears as a bright spot when it is positioned at the edge of the cell body in these polarization images (30). 50–100 such trajectories were analyzed to calculate the rotation frequency at each cell concentration.

RESULTS

Cells move in random directions in the absence of blue light (Fig. 1 *b*). The presence of blue light at one end of the chamber biases the movement of a majority of cells toward the light source (Fig. 1 *c*). However, a small but finite fraction of cells continue to move in directions other than the direction of the light source (Fig. 1 *c*). Probability density as a function of polar angle in the plane characterizes this phenomenon quantitatively (Fig. 1 *d*). The distribution is naturally peaked in the source direction with the peak height increasing with increase in light intensity (Fig. 1 *d*). To analyze the response of the system tractably, we define phototactic efficiency, ζ, as the fraction of cells that move in a direction $\pm 15^\circ$ of the source direction. At low

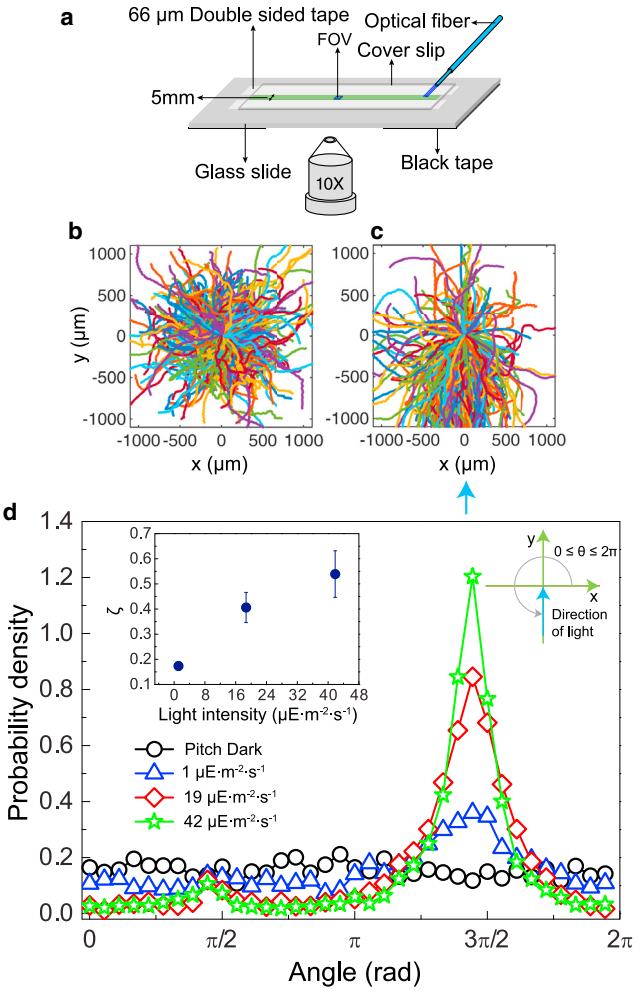

FIGURE 1 Experimental setup and phototactic response. (*a*) A schematic of the experimental setup is shown. (*b*) Trajectories of *C. reinhardtii* in pitch-dark condition at the cell concentration 5.3×10^5 cells cm^{-3} are shown. Each trajectory is arbitrarily colored for visual clarity. (*c*) Trajectories in the presence of light (19 $\mu E \cdot m^{-2} \cdot s^{-1}$) are shown. The blue arrow at the bottom of (*c*) shows the direction of stimulus light. In the pitch-dark condition, cell trajectories are uniform in all directions, whereas in the presence of light, a large fraction of cell trajectories are oriented toward the light source (positive phototaxis). (*d*) The probability density $P(\theta)$ for different light intensities according to the sign convention given at the top right corner in (*d*) is shown. (*Inset*) Phototactic efficiency ζ as a function of light intensity is shown. The error bars correspond to the SD of ζ. To see this figure in color, go online.

intensities of the light source, ζ is significantly less than 1 and approaches 1 at higher intensities (Fig. 1 *d*, *inset*).

Although the phototactic efficiency shows the anticipated increase with increasing light intensity, one expects that cell concentration will also play a role in governing phototaxis at the population level (23). Fig. 2, *a–d* show representative cell trajectories as a function of cell number density for a fixed light intensity. Starting from suspensions of a few cells, the peak height of the probability density decreases with increasing concentration until a critical concentration $\rho_c \approx 10^6$ cells cm^{-3} is reached. Above ρ_c, the peak height increases monotonically with the concentration (Fig. 2 *e*). This reentrant phototaxis behavior can equivalently be represented by the nonmonotonic variation of ζ with cell concentration (Fig. 2 *f*).

It could be reasonably expected that the measured probability distribution of trajectory orientations $\psi(\theta)$ could be captured by a self-propelled particle model (31). The simplest such model in this context would be that of noninteracting active Brownian particles subject to a polar aligning torque that tends to turn the trajectories of the particles along some particular direction in the lab frame. Let us pick this direction to be along $\theta = 0$. The Fokker-Planck equation governing the dynamics of the probability density $\psi(\theta, t)$ for the orientations of these self-propelled particles is given by the following:

$$\partial_t \psi(\theta, t) = D_R \partial_\theta^2 \psi + \frac{\gamma}{\xi_r} \partial_\theta (sin\theta \psi), \qquad (1)$$

where D_R is the rotational diffusion coefficient, γ is the torque strength, and ξ_r is the rotational friction coefficient. The steady-state solution to this equation is the well-known von Mises distribution function of the form $\psi(\theta) = (e^{\kappa cos\theta}/2\pi I_0(\kappa))$, where $\kappa = (\gamma/D_R)$ and I_0 is modified Bessel's function of the first kind. The experimentally obtained probability density as a function of polar angle is well fit by the von Mises distribution (Fig. 3 *a*). The density dependence of this probability distribution can now arise either through D_R, implying that the rotational diffusion and hence the characteristic decorrelation time of the orientational autocorrelation function depends on density, or through the torque γ. The experimental data reveal that this decorrelation time is independent of cell concentration (Fig. 3 *a*, *inset*; Fig. S2). Therefore, one can extract an effective density-dependent torque acting on the cells by fitting the experimental distribution to the von Mises distribution. The variation of best-fit values of γ with cell concentration (Fig. 3 *b*) is qualitatively similar to that of the model independent phototactic efficiency ζ (Fig. 2 *f*). Therefore, the reentrant behavior of the phototactic efficiency as a function of density is reliably captured by modeling this collective phenomenon as an effective density-dependent torque on each cell. Our results are consistent with previous studies of collective phototaxis in *Chlamydomonas* (23). It is notable that in these studies, the increase in polar order was found only in the presence of light and not in dark conditions. The notion of phototaxis efficiency used here is the same as that of polar ordering but serves as a better metric, modeled as a density-dependent torque, to capture the low-density behavior and identify its reentrant nature as a function of density.

Now, we seek to understand the mechanisms that underlie nontrivial behavior of the phototactic efficiency with concentration. The first feature of the efficiency in Fig. 2 *f* is a decrease with increasing densities at low densities. The fact that the rotational diffusion coefficient D_R is independent of density indicates that this decrease is not due to cell-cell scattering. But the presence of other cells at low densities can cause significant self-shading by absorbing the limited number of available photons, a behavior well captured by Beer-Lambert's law and known to be significant

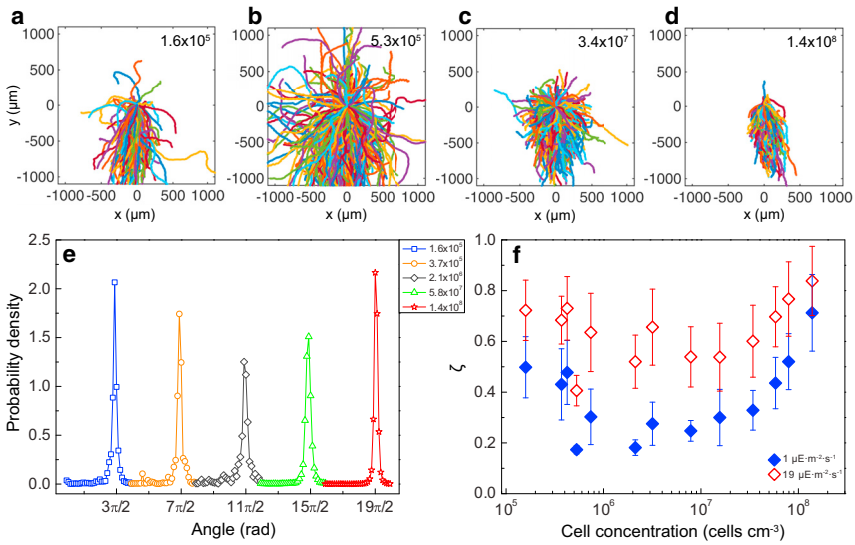

FIGURE 2 Phototactic efficiency is reentrant with the cell concentration. (*a–d*) Typical cell trajectories of *C. reinhardtii* under fixed light intensity (19 μE • m^{-2} • s^{-1}) with varying cell concentration (legend in unit of cells cm^{-3}) are shown. (*e*) The probability density $P(\theta)$ under fixed light intensity (19 μE • m^{-2} • s^{-1}) for increasing cell concentration is shown. The angle θ has been offset by multiples of 2π to shift the peak position for clarity. The height of the peaks quantifies the reentrant behavior of phototactic efficiency (legend in unit of cells cm^{-3}). (*f*) Phototactic efficiency ζ as a function of cell concentration corresponding to two different light intensities is shown. The error bars correspond to the SD of ζ. Phototactic efficiency decreases with increasing cell concentration until a critical concentration (ρ_c) is reached, above which phototactic efficiency increases with cell concentration. The dependence of phototactic efficiency on cell concentration is stronger at the lower light intensities. To see this figure in color, go online.

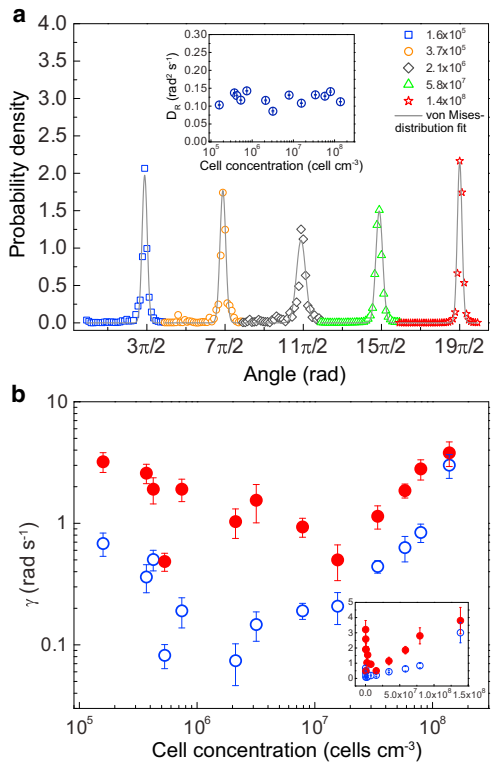

FIGURE 3 A self-propelled particle model for collective phototaxis. (*a*) Shown is a fit of the experimental probability densities (Fig. 2 *e*) to von Mises distribution, $\psi(\theta) = (e^{\kappa\cos\theta}/2\pi I_0(\kappa))$, where $\kappa = (\gamma/D_R)$ with rotational diffusion coefficient D_R, 0.13 rad^2 s^{-1}. The angle θ has been offset by multiples of 2π to shift the peak position for clarity (legend in units of cells cm^{-3}). (*Inset*) A plot of rotational diffusion coefficient, D_R, with the cell concentration shows that D_R is independent of the cell concentration. (*b*) A log-log plot of torque strength γ as a function of cell concentration under two different light intensities 1 μE • m^{-2} • s^{-1} (*open circle*) and 19 μE • m^{-2} • s^{-1} (*solid circle*) is shown. The error bars correspond to the SD of γ. The reentrant phototaxis behavior observed in the experiment can be effectively captured by a density-dependent aligning torque. (*Inset*) A linear representation of the same data is shown. To see this figure in color, go online.

for a variety of phototactic organisms (25,32–35). Therefore, the light sensing of the eyespot of any given cell is inhibited by the presence of other cells in its vicinity because of the absorption of light. If this is indeed the case, then we should also expect that this effect will be less prominent as we increase the light intensity because the abundance of photons will render the role of absorption insignificant. This is indeed consistent with our experimental data, rendering plausible our hypothesis of the role of self-shading in lowering the efficiency (Fig. 2 *f*). The increase in ζ at densities greater than the critical concentration however is more puzzling. It may be reasonable to postulate that the primary effect of high densities on the behavior of a single cell is that it slows down, and that is indeed the case in our experiments (Fig. 4 *a*; Figs. S3 and S5) (We do not know precisely the mechanism underlying the phenomenology of the density-dependent swim speed. Hydrodynamic and steric interactions could be possible mechanisms for decrease in cell speed with increase in density). This has been referred to as density-dependent motility in the context of the active matter literature (36,37). This could potentially affect the phototactic efficiency because of how CR cells detect light. The cells follow a helical trajectory because of cell body rotation. The cell body rotation allows the cell to collect photons from all directions in space. A decrease in linear speed implies a decrease in cell body rotation rate, which enables the cell to collect more photons per unit time and therefore detect the light direction more accurately (Fig. 4 *d*; Fig. S4) (We note that the decreased rotation rate also implies that the period of darkness is also higher, i.e., the time between detection events is longer. But our results nonetheless show an enhancement in phototactic efficiency).

One way to possibly validate this postulated mechanism for the increase in ζ as density increases beyond ρ_c would be to slow the cells down without changing the concentration of cells. One of the simplest ways to achieve that is to add polymer to the suspension medium, which increases the drag force on the cells, thereby lowering their speed. We use varying concentrations of methylcellulose to tune the speed of the cells keeping cell concentration fixed (Fig. 4 *b*). We find that ζ increases with increase in methylcellulose concentration, confirming the hypothesis that the observed increase in ζ with increasing cell concentration is mainly due to the lowering of cell speed (Fig. 4 *c*).

DISCUSSION

To summarize, we find that phototactic efficiency of CR cells is reentrant in going from a low-density dilute regime to a high-density collective one wherein dilute suspensions have smaller efficiency than that of single-cell limit, and dense suspensions have the opposite trend. We have identified the mechanism of enhanced efficiency in the collective regime to be the decrease in linear speed of the cells as the concentration increases. We speculate that decrease in linear speed leads to a decrease in rotational speed of the cells that enables them to sense the light direction more accurately.

The cell speed is nearly independent of concentration below the threshold concentration that marks the crossover between the individual and collective behavior. Therefore, the mechanism for decrease in efficiency with increasing cell concentration in the dilute regime is likely to be self-shading or some other form of hydrodynamic or steric interaction. It also remains to be explored how tightly the single-cell response is coupled with its collective response, namely, how chemical or genetic modifications that alter the single-cell phototaxis efficiency affect the collective behavior of such modified cells.

Complexity is common in biological systems, and its origin is often difficult to identify. Our results have demonstrated a rather simple physical and phenomenological mechanism underlying the observed complexity in the collective phototaxis of CR cells. Apart from identifying a

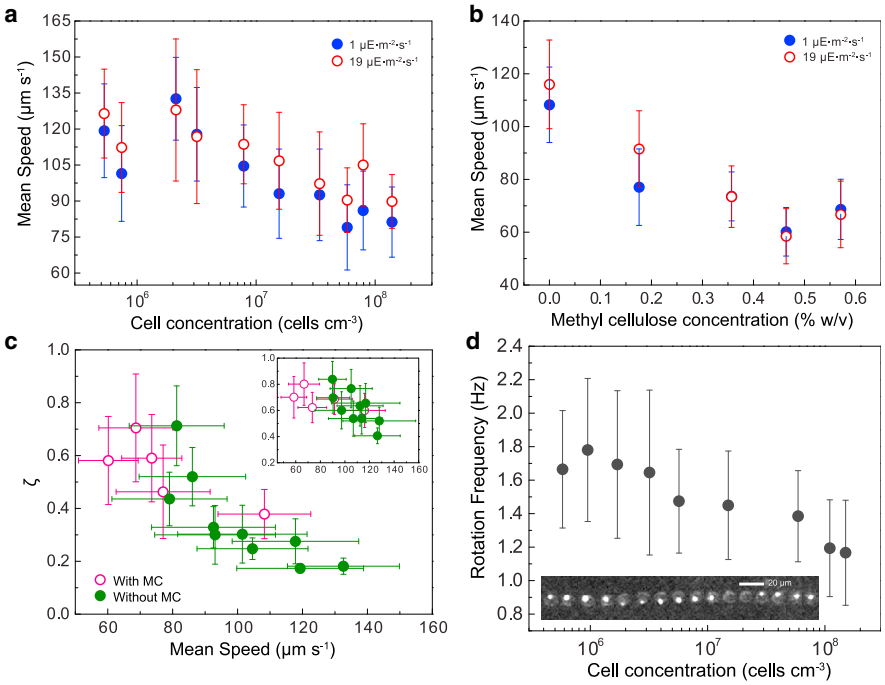

FIGURE 4 Physical origin of reentrant phototactic efficiency. (*a*) The mean speed as a function of cell concentration near and above critical concentration (ρ_c) is shown. As cell concentration increases, cells slow down. (*b*) The mean speed as a function of methyl cellulose concentration at a constant cell concentration 2.9×10^6 cells cm^{-3} is shown. The cell's speed was slowed down using methyl cellulose in the suspension medium. (*c*) Phototactic efficiency ζ as a function of the cell's mean speed at the intensity 1 $\mu E \cdot m^{-2} \cdot s^{-1}$ is shown. The pink open circle corresponds to the phototactic efficiency when cells are slowed down using methyl cellulose, and the green solid circle corresponds to the phototactic efficiency when the cell's speed was varied by cell concentration. In both the cases, phototactic efficiency decreases as the cell's speed increases. Phototactic efficiency is controlled by the mean speed. (*Inset*) Phototactic efficiency ζ as a function of the cell's mean speed at the intensity 19 $\mu E \cdot m^{-2} \cdot s^{-1}$ is shown. (*d*) The frequency of cell body rotation as a function of cell concentration in pitch-dark condition is shown. The decrease in the cell body rotation frequency with the cell concentration verifies the inference that the slower cells turn slowly. (*Inset*) A time-lapse (polarization) image showing a typical trajectory of a cell with the rotation frequency ~2 Hz in pitch dark at 33 frames per second is shown. Error bars in all the plots correspond to the SD of respective physical quantities. To see this figure in color, go online.

particular phenomenology associated with phytoplanktons with a single eyespot, this work can serve as a paradigm for the analysis of collective motility and taxis in microorganisms in general and perhaps motivate the design of control algorithms in collective robotics.

SUPPORTING MATERIAL

Supporting Material can be found online at https://doi.org/10.1016/j.bpj.2019.09.016.

AUTHOR CONTRIBUTIONS

A.B. and P.S. designed the research. S.K.C. carried out the experiments and associated analysis. All authors wrote the article.

ACKNOWLEDGMENTS

A.B. acknowledges support from the Brandeis Center for Bioinspired Soft Materials, NSF/MRSEC, DMR-1420382, and the hospitality of IISc and IMSc where part of this work was completed. S.K.C. acknowledges support from the DST-INSPIRE fellowship. This work was supported by the Wellcome Trust/DBT India Alliance Fellowship (grant no. IA/I/16/1/502356) awarded to P.S.

REFERENCES

1. Parrish, J. K., S. V. Viscido, and D. Grünbaum. 2002. Self-organized fish schools: an examination of emergent properties. *Biol. Bull.* 202:296–305.
2. Sumpter, D. J. T. 2010. Collective Animal Behavior. Princeton University Press, New Jersey.
3. Kearns, D. B. 2010. A field guide to bacterial swarming motility. *Nat. Rev. Microbiol.* 8:634–644.
4. Martinez-Corral, R., J. Liu, …, J. Garcia-Ojalvo. 2018. Bistable emergence of oscillations in growing *Bacillus subtilis* biofilms. *Proc. Natl. Acad. Sci. USA.* 115:E8333–E8340.
5. Zhang, R., L. Turner, and H. C. Berg. 2010. The upper surface of an *Escherichia coli* swarm is stationary. *Proc. Natl. Acad. Sci. USA.* 107:288–290.
6. Copeland, M. F., S. T. Flickinger, …, D. B. Weibel. 2010. Studying the dynamics of flagella in multicellular communities of *Escherichia coli* by using biarsenical dyes. *Appl. Environ. Microbiol.* 76:1241–1250.
7. Be'er, A., H. P. Zhang, …, H. L. Swinney. 2009. Deadly competition between sibling bacterial colonies. *Proc. Natl. Acad. Sci. USA.* 106:428–433.
8. Zhang, H. P., A. Be'er, …, H. L. Swinney. 2010. Collective motion and density fluctuations in bacterial colonies. *Proc. Natl. Acad. Sci. USA.* 107:13626–13630.
9. Bhaya, D., K. Nakasugi, …, M. S. Burriesci. 2006. Phototaxis and impaired motility in adenylyl cyclase and cyclase receptor protein mutants of Synechocystis sp. strain PCC 6803. *J. Bacteriol.* 188:7306–7310.
10. Ng, W. O., A. R. Grossman, and D. Bhaya. 2003. Multiple light inputs control phototaxis in Synechocystis sp. strain PCC6803. *J. Bacteriol.* 185:1599–1607.
11. Deforet, M., D. van Ditmarsch, …, J. B. Xavier. 2014. Hyperswarming adaptations in a bacterium improve collective motility without enhancing single cell motility. *Soft Matter.* 10:2405–2413.
12. Caiazza, N. C., R. M. Shanks, and G. A. O'Toole. 2005. Rhamnolipids modulate swarming motility patterns of *Pseudomonas aeruginosa*. *J. Bacteriol.* 187:7351–7361.
13. Welch, R., and D. Kaiser. 2001. Cell behavior in traveling wave patterns of myxobacteria. *Proc. Natl. Acad. Sci. USA.* 98:14907–14912.

14. Taylor, R. G., and R. D. Welch. 2008. Chemotaxis as an emergent property of a swarm. *J. Bacteriol.* 190:6811–6816.
15. Feinleib, M. E. H., and G. M. Curry. 1967. Methods for measuring phototaxis of cell populations and individual cells. *Physiol. Plant.* 20:1083–1095.
16. Feinlib, M. E. H., and G. M. Curry. 1971. The relationship between stimulus intensity and oriented phototactic response (topotaxis) in Chlamydomonas. *Physiol. Plant.* 25:346–352.
17. Arrieta, J., A. Barreira, …, I. Tuval. 2017. Phototaxis beyond turning: persistent accumulation and response acclimation of the microalga Chlamydomonas reinhardtii. *Sci. Rep.* 7:3447.
18. Goldstein, R. E. 2015. Green algae as model organisms for biological fluid dynamics. *Annu. Rev. Fluid Mech.* 47:343–375.
19. Giometto, A., F. Altermatt, …, A. Rinaldo. 2015. Generalized receptor law governs phototaxis in the phytoplankton Euglena gracilis. *Proc. Natl. Acad. Sci. USA.* 112:7045–7050.
20. Drescher, K., R. E. Goldstein, and I. Tuval. 2010. Fidelity of adaptive phototaxis. *Proc. Natl. Acad. Sci. USA.* 107:11171–11176.
21. Stavis, R. L., and R. Hirschberg. 1973. Phototaxis in Chlamydomonas reinhardtii. *J. Cell Biol.* 59:367–377.
22. Dolle, R., J. Pfau, and W. Nultsch. 1987. Role of calcium ions in motility and phototaxis of Chlamydomonas reinhardtii. *J. Plant Physiol.* 126:467–473.
23. Furlan, S., D. Comparini, …, B. Mazzolai. 2012. Origin of polar order in dense suspensions of phototactic micro-swimmers. *PLoS One.* 7:e38895.
24. Harris, E. H., D. B. Stern, and G. B. Witman. 2009. The Chlamydomonas Sourcebook, Second Edition. Academic Press, London.
25. Foster, K. W., and R. D. Smyth. 1980. Light antennas in phototactic algae. *Microbiol. Rev.* 44:572–630.
26. Ueki, N., T. Ide, …, K. Wakabayashi. 2016. Eyespot-dependent determination of the phototactic sign in Chlamydomonas reinhardtii. *Proc. Natl. Acad. Sci. USA.* 113:5299–5304.
27. Jékely, G., J. Colombelli, …, D. Arendt. 2008. Mechanism of phototaxis in marine zooplankton. *Nature.* 456:395–399.
28. Rüffer, U., and W. Nultsch. 1991. Flagellar photoresponses of Chlamydomonas cells held on micropipettes: II. Change in flagellar beat pattern. *Cell Motil. Cytoskelet.* 18:269–278.
29. Smyth, R. D., and H. C. Berg. 1982. Change in flagellar beat frequency of Chlamydomonas in response to light. *Prog. Clin. Biol. Res.* 80:211–215.
30. Kamiya, R., and G. B. Witman. 1984. Submicromolar levels of calcium control the balance of beating between the two flagella in demembranated models of Chlamydomonas. *J. Cell Biol.* 98:97–107.
31. Hancock, B., and A. Baskaran. 2015. Effect of reorientation statistics on torque response of self-propelled particles. *Phys. Rev. E Stat. Nonlin. Soft Matter Phys.* 92:052143.
32. Ghorai, S., and N. A. Hill. 2005. Penetrative phototactic bioconvection. *Phys. Fluids.* 17:074101.
33. Shigesada, N., and A. Okubo. 1981. Analysis of the self-shading effect on algal vertical distribution in natural waters. *J. Math. Biol.* 12:311–326.
34. Huesemann, M. H., J. Van Wagenen, …, B. Crowe. 2013. A screening model to predict microalgae biomass growth in photobioreactors and raceway ponds. *Biotechnol. Bioeng.* 110:1583–1594.
35. Pottier, L., J. Pruvost, …, C. G. Dussap. 2005. A fully predictive model for one-dimensional light attenuation by Chlamydomonas reinhardtii in a torus photobioreactor. *Biotechnol. Bioeng.* 91:569–582.
36. Cates, M. E., and J. Tailleur. 2015. Motility-induced phase separation. *Annu. Rev. Condens. Matter Phys.* 6:219–244.
37. Cates, M. E., D. Marenduzzo, …, J. Tailleur. 2010. Arrested phase separation in reproducing bacteria creates a generic route to pattern formation. *Proc. Natl. Acad. Sci. USA.* 107:11715–11720.